Journal of Heat and Mass Transfer Research

Journal homepage: https://jhmtr.semnan.ac.ir

Semnan University

ISSN:2383-3068

Research Article

Design and Analysis of Helical Cone Coil Heat Exchanger for Low Grade Heat Recovery

Ajay Hundiwale [a], Lokpriya Gaikwad [a*], Sandeep Joshi [b]

[a] *Department of Mechanical Engineering, SIES Graduate School of Technology, Nerul, Navi Mumbai, 400706, India*

[b] *Department of Mechanical Engineering, Pillai College of Engineering, New Panvel, 410206, India*

ARTICLE INFO

Article history:

Received: 2024-03-17

Revised: 2024-06-29

Accepted: 2024-08-21

Keywords:

Low-grade heat recovery;

Shell and helical cone coil heat exchanger;

Dual cylinder diesel engine;

Overall heat transfer coefficient.

ABSTRACT

The recovery of low-grade heat is crucial for energy conservation, particularly in manufacturing and process industries that discharge substantial waste energy into the atmosphere. This waste heat, varying from slightly above room temperature to several hundred degrees Celsius, can exist as liquids, gases, or a combination of both. Low-grade heat recovery, also known as waste heat recovery, involves capturing and transferring this energy using gas or liquid mediums, reintroducing it into the process as an additional energy source. This process is essential for improving energy efficiency and promoting sustainability, employing various techniques tailored to the waste heat temperature. Helical cone coils offer significantly enhanced heat transfer characteristics compared to straight tubes. These coils feature a secondary fluid flow running in planes parallel to the primary flow within their helical structure. This study focuses on designing and analyzing a shell and helical cone coil heat exchanger, highlighting its ability to reduce unit size compared to a standard shell-and-tube heat exchanger operating under the same thermal load. The experimental setup included a shell and helical cone coil configuration, utilizing diesel engine exhaust as the hot gas source and tap water as the cold fluid in a counterflow arrangement. The investigation revealed that helical cone coils extracted 15 to 20% more heat compared to conventional straight tubes, demonstrating improved effectiveness and compactness.

1. Introduction

The process of recovering and reprocessing thermal energy that would otherwise be lost to the atmosphere is known as low-grade heat recovery. Efficiency is a critical performance metric for diesel engines. Exhaust gas loss significantly impacts engine performance. Low-grade heat recovery, also known as waste heat recovery (WHR), often eliminates or reduces the need for additional fuel energy input. WHR systems are extensively used in industrial and chemical industries as heat exchangers for various applications, including refrigeration, air conditioning systems, and food processing. Therefore, the demand for high-performance heat exchangers is crucial for energy conservation.

During the analysis of numerous heat exchanger designs, it has been observed that shell and tube configurations of various shapes are commonly used in various industries. According to several studies, helical coiled tubes

*** Corresponding author.**
E-mail address:lokpriya2007@gmail.com

Cite this article as:

Hundiwale, A., Gaikwad, L. and Joshi, S., 2025. Design and Analysis of Helical Cone Coil Heat Exchanger for Low Grade Heat Recovery. *Journal of Heat and Mass Transfer Research*, 12(1), pp. 61-72.

https://doi.org/10.22075/JHMTR.2024.33519.1533

perform similarly to straight cylinders in terms of heat transfer effectiveness [1, 2]. Helical coiled tubes in heat exchangers find applications across diverse industrial sectors such as oil refining, refrigeration, HVAC (Heating, Ventilation, and Air Conditioning), food processing, nuclear industries, and space exploration [3]. Spiral tube heat exchangers are valued for their high overall heat transfer coefficient, excellent efficiency, compact size, and other advantages. Additionally, the helical design allows for handling high temperatures and significant temperature variations without the need for expensive expansion joints or high-stress levels. Spiral tubes are also effective in managing high-pressure fluids, and research indicates that fouling in spiral tubes is minimal under conditions of high turbulence.

In the steel industry, gases from various industrial processes are typically used as a low-grade heat source. Using flat heat pipes (FHP), it has been observed that up to 15.6 kW of power can be recovered from a source temperature of 450°C [4]. In this experiment, a prototype of an innovative FHP model, measuring 1 meter in length and 1 meter in width, was fabricated and evaluated. A shell and pancake-type heat exchanger designed for low-grade heat recovery from producer gas was fabricated and tested [5]. The experiment involved using pancake-shaped stainless-steel tubes within a mild steel shell. The flow rate of the hot liquid remained constant throughout the experiment. Pancake-style tubes were employed for the cold fluid (water), while the shell accommodated the hot fluid (engine exhaust gas). Heat transfer coefficients for water and gas were determined, revealing that theoretical and experimental values aligned closely, with an accuracy of approximately 8%. In another study, E. Gholamalizadeh [6] focused on improving heat transfer in helically coiled tube heat exchangers by incorporating coiled wire inserts with varying cross-sections and sizes. This research analyzed the Nusselt number and friction factor between smooth coiled tubes and those with wire inserts, demonstrating enhancements with specific cross-sectional wire designs.

Alimoradi et al. [7] investigated the fundamental mathematical boundaries and optimal configurations for heat exchangers utilizing shells and helically wound tubes. They calculated various dimensionless geometric parameters and experimental coefficients to enhance heat transfer efficiency. Purandare et.al. [8] conducted a study on the impact of heat transfer using various tube geometries, including spiral, helical, and conical tube heat exchangers. Throughout the experiment, a detailed investigation was carried out to understand how the heat transfer rate shifts as the fluid transitions from spiral to helical geometry. Additionally, Purandare et. al. [8] studied the impact of flow intensity using various tube geometries such as twisted, helical, and cone-shaped heat exchangers. Their experiments provided insights into how heat transfer rates vary as fluid flow transitions from spiral to helical configurations.

A conical helical coil heat exchanger was fabricated, as reported by [9]. The experiment aimed to determine the overall Heat Transfer Coefficient (OHTC) while adjusting the mass flow rates of water, with a constant gas mass flow rate maintained. Predicted values for water outlet temperature showed a deviation ranging from -8.20% to 30% compared to expected values. In another study, [10] investigated a cone-shaped helically coiled heat exchanger using both experimental and numerical approaches. Computational fluid dynamics (CFD) simulations were employed to model laminar and turbulent flows of an incompressible fluid, specifically water. An empirical correlation for the average Nusselt number was derived from experimental data, indicating a maximum variation of 23% throughout the study. The experimental data were used to validate the numerical simulations, showing agreement within 30% between the two. The use of porous filling is recognized as an effective method to enhance heat transfer rates in heat exchangers, aimed at improving their efficiency. In a recent study [11], a numerical investigation was conducted to evaluate heat transfer performance and pressure drop in various porous-filled STHXs (Shell-and-Tube Heat Exchangers). The findings demonstrated that porous-filled designs significantly mitigated thermal gradients observed in conventional STHXs, resulting in more uniform thermal distribution. Furthermore, the heat transfer efficiency of porous-filled configurations increased by up to 60% compared to conventional types; however, this improvement was accompanied by higher pressure drop values.

The impact of geometric parameters of an immersed helical condenser coil on heat transfer characteristics and water velocity distribution during the water heating process was studied by [12]. After validating the numerical model with experimental data, the effects of coil parameters on water velocity distribution were examined. This investigation aims to provide guidance for optimizing the condenser coil structure for efficient water heating processes. The investigation on the influence of condenser coil

designs on the heat transfer process of a helical coil heat exchanger immersed in a storage tank was carried out by Sami Missaoui et al. [13]. The experimental results showed that the numerical model proposed in this study closely matched the experimental data, with a deviation of ±1.6%. Furthermore, the impact of the main geometrical parameter on the overall heat transfer coefficient and water temperature distribution was examined. It was observed that both temperature distribution and overall heat transfer coefficient increase with the number of pipe turns in a helically coiled tube heat exchanger.

[14,15,16] Studied the thermal performance of a helical condenser coil compared to other geometrical shapes of condenser coil designs. By modifying the coil shape, this investigation offers guidance to optimize the coil structure for refrigeration machines used in domestic hot water production. A study was conducted on a heat pump water heater using immersed helically coiled tubes by Sami Missaoui et al. [17]. The investigation focused on the effects of storage tank dimensions and copper coil pitch on the heating process. The evolution of temperature and velocity fields on the waterside at the axial centerline of the cylindrical water tank was analyzed. During the investigation, it was observed that the simulation results closely matched the experimental findings.

The existing literature extensively covers experimental and numerical data on helical coil heat exchangers. However, there is a noticeable gap in research regarding helical cone coil and shell heat exchangers from thermodynamic perspectives, particularly in the context of recovering waste heat in the medium temperature range (100-400°C). Therefore, the primary objective of this study is to design and evaluate a shell-integrated helical cone coil heat exchanger. The aim is to optimize the contact area between the tube side and the shell-side fluid, with the goal of achieving superior heat recovery compared to traditional heat exchangers. Additionally, the research focuses on reducing the overall size while maintaining the heat extraction capacity equivalent to conventional systems.

2. Design of Helical Cone Coil Heat Exchanger

The heat exchanger's configuration is deliberately organized to facilitate the flow of a single fluid through a helical cone coil tube. This plan guarantees the unidirectional development of one liquid through the shell side and the other through the curl side. With the goal of optimizing heat recovery and utilizing the available surface area within the shell, the coils are strategically positioned to act as a diffuser for the shell-side fluid. The conical shape also generates a secondary flow, maximizing the heat transfer process and creating an arrangement that enhances heat extraction from the system. The main focus is on developing a suitable heat exchanger for recovering sensible heat from various industrial processes involving medium-temperature low-grade heat. The considered working liquids are faucet water and hot vent gas obtained from a Twin-chamber diesel engine. Moreover, the design accepts that the hot pipe gas will be coordinated through the shell, while the progression of water will be worked with through the helical cone coil of the exchanger.

2.1. Geometrical Design

For the aim of the experiment, a unique sort of heat exchanger with a helical cone coil is being designed. To recover waste heat from the exhaust gas, the experimental model will be coupled with a dual-cylinder diesel engine with a 5 kW capacity. The winding construction of helical curls frustrates the assembling of helical cone loops utilizing coil wrapping hardware. To make the creation interaction practical, a wooden model is made to wind the curl into a specific shape. By considering the manufacturing constraints, the cone angle (2α) was decided.

Seamless stainless-steel tube of ¾" was used to fabricate helical cone coil. The pitch of the helical cone coil will be the outer diameter of the SS tube. By considering TEMA standards MS pipe of 50 cm length and OD 12.75 inch was used to fabricate shell. It is finalized that the hot exhaust gases will be circulated from the shell and the cold water will flow from the helical cone coil.

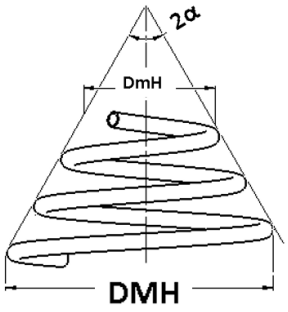

Fig. 1. Helical Cone Coil configuration

According to the diameter and length of the shell, the big and small diameters of the helical cone coil were decided. Water enters from one side of the Helical cone coil and leaves from the other side, and hot exhaust gas flows from the shell. The hot exhaust gas and cold-water flows

in a counterclockwise direction (See figures 1 to 3). From the wooden model and effective length of shell number of turns in the helical cone coil, Nc was calculated. The pitch of the coil was considered as the outer diameter of tube, so the total length of the Helical cone coil was calculated as

$$L_{CC} = \sqrt{(\pi \times DH \times N_c)^2 - (Pitch \times N_c)^2} \quad (1)$$

The curvature ratio, δ, of the coil is.

$$\delta = \frac{d_i}{DH} \quad (2)$$

The area of the cone is

$$A_c = \left[\left(\frac{\pi \times DMH \times S_h}{2} + \frac{\pi \times DMH^2}{4}\right) - \left(\frac{\pi \times DmH \times s_h}{2} + \frac{\pi \times DmH^2}{4}\right)\right] - \left[\left(\frac{\pi \times D_1 \times S_h}{2} + \frac{\pi \times D_1^2}{4}\right) - \left(\frac{\pi \times d_1 \times s_h}{2} + \frac{\pi \times d_1^2}{4}\right)\right] \quad (3)$$

The area available for the flow of hot exhaust gases

$$A_{fl.g} = \left(\frac{\pi}{4} D_1^2 - A_c\right) \quad (4)$$

Area of flow of water is

$$A_{fl.g} = \frac{\pi}{4} d_i^2 \quad (5)$$

Also, the surface area of the shell can be calculated as

$$A_{ss} = \pi \times D_s \times L_s \quad (6)$$

2.2. Thermal Analysis

After the fabrication and assembly of the heat exchanger, the heat exchanger was installed with the dual-cylinder diesel engine in counter-flow arrangement to utilize the maximum exhaust heat in the available area of the heat exchanger. While installing, the Helical con coil arrangement was made in such a way that the helical cone coil would not act as a nozzle for exhaust gases. By heat balance equation,

Heat absorbed by the cold fluid = Heat rejected by the hot fluid

Here, the total heat carried by the combustion gases is.

$$Q_{eg} = m_{eg} \times Cp_{eg} \times (T_{eg.i} - T_{eg.o}) \quad (7)$$

$$\in = \frac{\text{Actual Heat Transfer}}{\text{Maximim possible heat transfer}} \quad (8)$$

$$= \frac{C_{eg} \times (T_{eg.i} - T_{eg.o})}{C_{min} \times (T_{eg.i} - T_{w.i})} \quad (9)$$

where C_{eg} and C_w are the heat capacities of exhaust gas and cold water, respectively. The heat lost by the exhaust gas is assumed to be absorbed by the water at the same flow rate in this case.

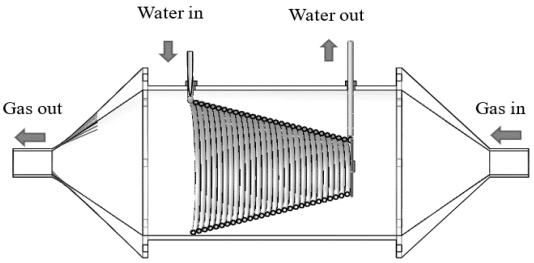

Fig. 2. CAD Model of Shell and Helical Cone Coil Heat Exchanger

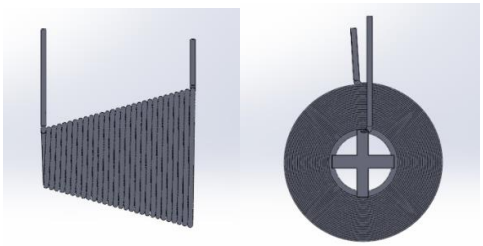

Fig. 3. CAD Model of Helical Cone Coil

$$V_{eg} = \frac{\dot{m}}{\rho_{eg} \times A_{f.eg}} \quad (10)$$

$$Re_{eg} = \frac{\rho_{eg} \times V_{eg} \times d_{out}}{\mu_{eg}} \quad (11)$$

The flow between banks of tubes for laminar and turbulent flow may be computed using an aligned tube configuration and the Richard et al. and Petukhov Equation.

$$Nu_{eg} = 0.192 \times Re_{eg}^{0.81} \times Pr_{eg}^{1/3} \quad (12)$$

Valid for 2000 < Reeg< 4000

$$Nu_{eg} = \frac{(\frac{f_{eg}}{8}) \times (Re_{eg} - 1000) \times Pr_{eg}}{1.07 + 12.7\,(\frac{f_{eg}}{8})^{0.5} \times (Pr_{eg}^{2/3} - 1)} \quad (13)$$

Valid for 0.5 < Preg< 2000

3000 < Reeg< 5000000

Similarly, the following equations may be applied on the water side. The computation of the Nusselt number for the water side fully developed flow can be calculated by using equation [13]

$$Nu_w = 0.00619 \times Re_w^{0.92} \times Pr_w^{0.4} \times (1 + 3.455\,\delta) \quad (14)$$

Valid for 5 × 10^3< Rew< 10^5

0.7<Prw< 5

0.0267 < δ <0.0884

and by using Grimson's correlation for flow across banks of tubes

$$Nu_w = 1.13 \times 0.374\,(R_e^{0.581}) \times Pr^{1/3} \qquad (15)$$

Valid for 2000 < Rew<4000

Tubes in water side heat transfer are Helical cone coils. Hence curvature ratio must be considered for such tubes. A secondary flow is also produced during the fluid flow due to centripetal force. The Dean number (De) indicates the relationship between centripetal force and tube curvature ratio. The following equation may be used to compute it.

$$De_w = \frac{\sqrt{\frac{1}{2}(\text{Inertia Fore}) \times (\text{Centripetal Force})}}{\text{Viscus Force}} = Re_w \times \sqrt{\frac{d_{in}}{DH}} \qquad (16)$$

Nusselt number can also be calculated by using the dean number for the Helical cone coil by the equation mentioned by [8]

$$Nu_{De} = 0.141 \times De^{0.80} \times Pr_w^{-0.187} \qquad (17)$$

Nusselt number values derived from Reynolds number and Dean number correlation must be about the same. The friction factor and tube side pressure drop will be computed as follows:

$$f_w = 2\,\frac{\Delta P}{L_{cc}} \times \frac{d_{in}}{\rho v^2} \qquad (18)$$

$$f_w = \frac{64}{Re_w} \qquad (19)$$

As a result, the total heat transfer coefficient based on outer surface area is calculated as

$$U_{out} = \frac{1}{\frac{1}{h_{in}} + \frac{d_{out}}{2k}\ln\frac{d_{out}}{d_{in}} + \frac{1}{h_{out}}\frac{d_{out}}{d_{in}}} \qquad (20)$$

For the single shell pass with multiple tube passes and flow counter-flow arrangement, LMTD can be calculated as

$$\Delta T_{lm} = \frac{(T_{eg.in} - T_{w.out}) - (T_{eg.out} - T_{w.in})}{\ln\frac{T_{eg.in} - T_{w.out}}{T_{eg.out} - T_{w.in}}} \qquad (21)$$

2.3. Experimentation

A dual-cylinder Kirloskar, Crompton Greaves water-cooled diesel engine with a rated speed of 1500 is utilized in the experiment. The experimental apparatus includes a shell and a heat exchanger with a helically wound cone coil. Care was taken throughout the manufacturing process to ensure the coils' dimensional stability. While constructing a heat exchanger that can successfully recover sensible heat from a variety of industrial processes, low-grade heat recovery at medium temperatures is taken into account (See figures 4 and 5). Working fluids include water and engine exhaust gas. Parameters considered for the analysis are provided in Table 1.

Table 1. Parameters considered for analysis.

Sr. #	Parameter	Details
1	Outer tube Diameter (do)	9.52 mm
2	Inner tube Diameter (di)	7.52 mm
3	Total Length of Tube	18 m
4	Pitch	do
5	Curvature ratio	0.036
6	Big diameter of cone	280 mm
7	Small diameter of cone	140 mm
8	Outer Diameter of shell (OD)	324mm
9	Inner Diameter of shell (ID)	304.8mm
10	Total Shell Length	500 mm
11	No of turns (n)	28

In the first place, water will be given to examine the exploratory arrangement and quest for fitting holes. After the assessment, standard water and fumes gas are allowed to travel through the helical cone coil side and the shell side, separately. The shell is made of steel (MS), while the helical cone coils are made of stainless steel tubes.

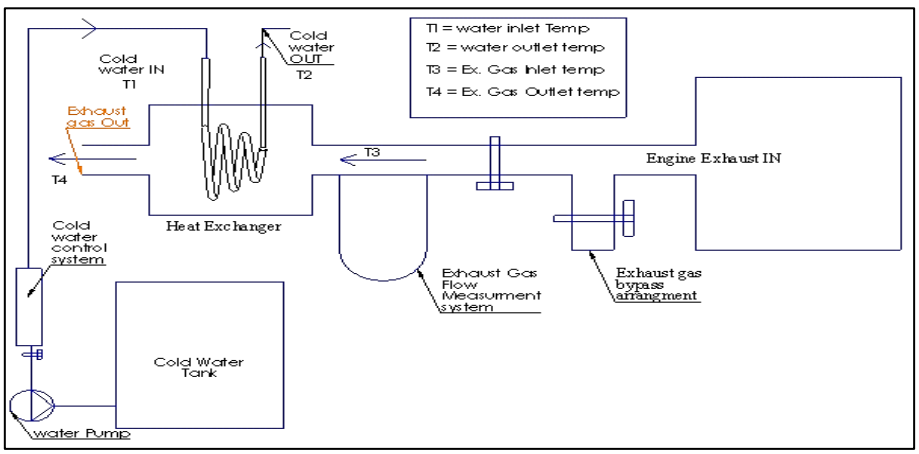

Fig. 4. Experimental setup of shell and helical cone coil heat exchange with dual cylinder diesel engine

Fig. 5. Shell and helical cone coil heat exchanger setup

The heat exchanger was fully assembled after the manufacturing and installation of the helical cone Coil. The arrangement included K-type thermocouples and a temperature indicator. A rotameter with a range of 0 to 5 LPM was also connected to monitor the water flow rate. Before being installed in the setup, the thermocouple and rotameter were calibrated. Conditions of turbulence and counter-flow were used throughout the tests that were carried out. Altering the flow rates of exhaust gas and water in an alternating fashion allows for equal measurements to be obtained. Allow the experiment to continue for 15–20 minutes or until the condition of steady state is reached, whichever comes first. The important reading is obtained for a range of different exhaust gas mass flow rates (0.67, 0.46, 0.32, and 0.17 kg/s), as well as water flow rates (1 to 5 lpm).

3. Error Analysis

In science and technology, experimental analysis is required to demonstrate physical principles and validate processes or systems. Different sources of errors come during experimental results. Coleman et al. [18] and ANSI/ASME "Measurement uncertainty" [19] proposed the uncertainty analysis for all experiments, and it was discovered by referring to Kannadasan et al. [20] that the experimental error is less than 10% for all runs.

a) Volume flow rate of water

Error in the measurement of the Volume flow rate of water by using a calibrated rotameter.

evol.fl = ± 0.1 m^3/s

b) Mass flow rate of exhaust gas

The mass flow rate of exhaust gas can be calculated by the following equation.

$\dot{m}_{hg} = \rho_{hg} \times \frac{\pi}{4} D^2 \times V_{hg}$

where ρ is the density of ex. gas, D is the diameter of the shell, and V is velocity of ex. gas.

Error in the measurement of diameter is

ed = ± 1 mm

Error in the measurement of Ex. gas velocity with the help of U tube manometer

hv = ± 5 mm

ev =±0.3 m/s (V= $\sqrt{2gh}$)

Error is propagated to calculate values due to errors in measuring devices. Error in calculation of mass flow rate of exhaust gas is as follows.

$$\Delta E\dot{m}_{hg} = \pm \sqrt{\left(\frac{\partial m_{hg}}{\partial v_{hg}} e_v\right)^2 + \left(\frac{\partial m_{hg}}{\partial d_s} e_d\right)^2} = 2.78\%$$

a) Reynolds number

$$Re = \frac{\rho \times V \times d}{\mu}$$

Error in the measurement of diameter is

ed = ± 1 mm

Error in the measurement of Ex. gas velocity with the help of U tube manometer

hv =± 5 mm and ev = ± 0.3 m/s (V= $\sqrt{2gh}$)

Error in the measurement of the volume flow rate of water with the help of rotameter

evol.fl = ± 0.1 m^3/s

Error in the measurement of water side and gas side Reynolds Number calculated as

$$\Delta ERe = \pm \sqrt{\left(\frac{\delta Re}{\partial v_{hg}} e_v\right)^2 + \left(\frac{\delta Re}{\partial d_s} e_d\right)^2} = \pm 2.48$$

b) Heat transfer

$$Q = m \times Cp \times \Delta T$$

The error in the measurement of temperature is ± 0.1 °C.

Error in the measurement of the volume flow rate of water with the help of rotameter

$$evol.fl = \pm 0.1\ m3/s$$

Error in the measurement of exhaust gas

$$\Delta E\dot{m}_{hg} = \pm\sqrt{\left(\frac{\partial m_{hg}}{\partial v_{hg}}e_v\right)^2 + \left(\frac{\partial m_{hg}}{\partial d_s}e_d\right)^2} = \pm 4.06$$

c) Nusselt Number

$$Nu = c \times Re^m \times Pr^n \times f$$

Error in the measurement of water side and gas side Reynolds Number calculated as

$$\Delta ERe = \pm\sqrt{\left(\frac{\delta Re}{\partial v_{hg}}e_v\right)^2 + \left(\frac{\delta Re}{\partial d_s}e_d\right)^2}$$

$$f = \frac{2\times\Delta P\times d}{L\times\rho\times v^2}$$

Error in the measurement of friction factor can be calculated as

$$\Delta Ef = \pm\sqrt{\left(\frac{\delta f}{\partial v_{hg}}e_v\right)^2 + \left(\frac{\delta f}{\partial l_s}e_l\right)^2 + \left(\frac{\delta f}{\partial d_s}e_d\right)^2 + \left(\frac{\delta f}{\partial \Delta P}e_{\Delta P}\right)^2}$$

Error in the measurement of Nusselt Number = ΔERe + ΔEf = ± 7.87

d) Dean Number

$$De = Re \times \sqrt{\frac{d_i}{2R}}$$

Error in the measurement of water side and gas side Reynolds Number calculated as

$$\Delta ERe = \pm\sqrt{\left(\frac{\delta Re}{\partial v_{hg}}e_v\right)^2 + \left(\frac{\delta Re}{\partial d_s}e_d\right)^2}$$

Error in the measurement of diameter is

$$ed = \pm 1\ mm = \pm 7.51$$

e) Heat Transfer Coefficient

$$h = \frac{Nu\times K}{L}$$

Error in the measurement of Nusselt Number = ΔERe + ΔEf

Error in the measurement of length is

$$el = \pm 1\ mm = \pm 7.90$$

f) LMTD

$$\Delta T_{lm} = \frac{(T_{hg.in} - T_{cw.out}) - (T_{hg.out} - T_{cw.in})}{\ln\frac{T_{hg.in}-T_{cw.out}}{T_{hg.out}-T_{cw.in}}}$$

The error in the measurement of temperature is ± 0.1 °C.

Error calculated in LMTD = ± 3.23.

The detailed error analysis is shown in Table 2.

Table 2. Error analysis.

Sr #	Quantity	% Uncertainty
1	Volume flow rate water	1.56
2	Mass flow rate exhaust gas	2.78
3	Reynolds number (Re)	2.48
4	Heat transfer	4.06
5	Heat transfer coefficient	7.90
6	LMTD	3.23
7	Nusselt number (Nu)	7.87
8	Dean number (De)	7.51

4. Results and Discussion

Several trials have been carried out for various mass flow rates of water and exhaust gases. To regulate the mass flow rate of exhaust gas, a U tube manometer and gate valves are attached to the setup. Water flow rates ranging from 1.0 lpm to 3.5 lpm and exhaust gas side mass flow rates ranging from 0.67 to 0.17 kg/s were measured.

4.1. Effect of Flow Rate on Qe

Testing indicated a significant decline in the Heat Exchanger's performance at lower gas mass flow rates. The experimental data are presented graphically with four lines representing different gas mass flow rates: 0.73 kg/s, 0.50 kg/s, 0.35 kg/s, and 0.18 kg/s. As can be seen in Figure 6, the maximum amount of heat recovered occurs at an exhaust gas mass flow rate of 0.73 kg/s. The observed trend suggests that as the water mass flow rate increases, the heat extracted for each gas flow rate remains relatively stable or shows a slight increase.

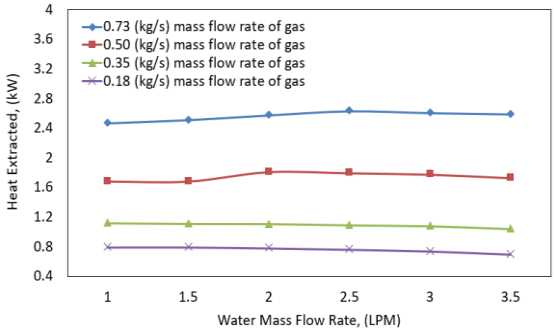

Fig. 6. Heat extracted at different mass flow rates of water and at different mass flow rates of gases.

This implies that the heat extraction from the gas depends on the gas flow rate, and increasing the water flow rate does not significantly affect the heat extraction rate. When hot fluid passes through a shell, and cold fluid flows through a helical cone tube, the tube's shape causes secondary flows to form, influencing heat transfer. These secondary flows involve swirling or cross-stream motion alongside the main axial flow of the fluids. They improve mixing between the hot and cold fluids, disrupting the thermal boundary layers near the tube wall and enhancing heat transfer efficiency. The swirling motion brings fresh fluid into contact with the tube wall, thereby increasing the heat transfer coefficient.

In a helical cone coil, secondary flow is more pronounced at larger diameters due to the coil's curvature and greater centrifugal forces. This enhances secondary flow patterns, particularly in regions where the tube diameter is larger. These secondary flows alter the local heat transfer coefficient along the helical cone tube, resulting in higher heat transfer rates where the secondary flow is intensified. This configuration facilitates more efficient thermal energy transfer between the hot and cold fluids compared to scenarios with minimal secondary flow. In general, the heat extracted by water in a helical cone coil is greater than that extracted by water in a traditional shell and tube heat exchanger. This is because the area of the helical cone coil heat exchanger and the total tube length of the helical cone coil heat exchanger are both greater, and the optimum area of the helical cone coil is out to the hot exhaust gas flow.

4.2. Effect of Re on Effectiveness, ϵ

During testing, it was observed that as the mass flow rate of water increases, the rate of heat extraction decreases. This phenomenon could be attributed to several factors. Firstly, the contact time between the exhaust gas and water increases as the effective area for water flow expands. Additionally, the helical cone coil generates secondary flow, which enhances heat transfer rates compared to traditional shell-and-tube heat exchangers.

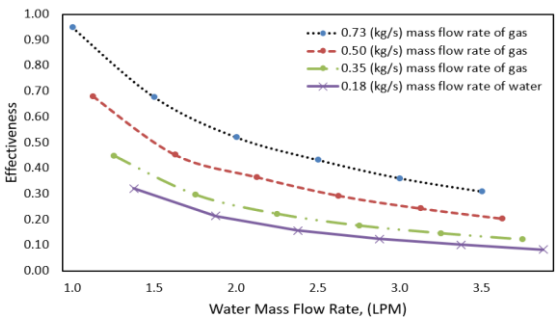

Fig. 7. Effectiveness vs. Reynolds Number for different mass flow rates of exhaust gases

Analysis indicates that at low mass flow rates of water (low Re), there is a significant percentage variation in effectiveness concerning the tube side flow rate. However, at higher mass flow rates (high Re), this variation decreases. Figure 7 illustrates that as the water flow rate decreases, the heat exchanger's effectiveness improves. This efficiency enhancement is due to prolonged contact between hot gas and cold water compared to conventional shell-and-tube heat exchangers.

Moreover, the curvature of the helical cone coil induces centrifugal force, leading to the development of secondary flow. This curvature effect causes water to move faster on the outer side of the coiled tube than on the inner side. The impact of secondary flow patterns on both the Reynolds number and heat exchanger effectiveness is substantial. Increased secondary flow on the tube side enhances mixing and elevates heat transfer rates within the coil. This higher flow rate boosts the convective heat transfer coefficient by improving mixing and reducing thermal boundary layers, thereby enhancing overall heat transfer efficiency. However, secondary flows also result in higher pressure drops, which increase pumping costs and affect overall efficiency.

Increases in tube side flow rate are accompanied by increases in Nu (Re). This is likely due to an increase in the velocity of the tube side fluid, intensifying the secondary currents formed within the coiled tube. These secondary currents arise from the centrifugal force exerted on fluid particles moving through a curved tube. They facilitate fluid mixing by reducing the thickness of the laminar boundary layer along the flow path and shortening its overall length.

4.3. Nu – De Correlation

There are numerous studies on helical coil configuration in the literature. The comparison of the Nu value predicted in this work and the Nu predicted in the literature [8] with the Dean number shows that they are in good agreement.

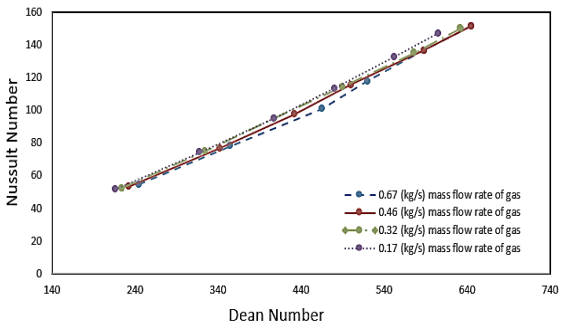

Fig. 8. Nusselt number vs. Dean number at different mass flow rates of exhaust gases

The correlation between the Nusselt number and the Dean number is parallel throughout the experiment, as shown in figure 8. That could explain why the Nusselt number correlation with Reynolds number and the Nusselt number correlation with Dean number for the water side have similar values.

Figure 9 shows that the heat recovery rate observed in actual experimentation exceeds theoretical predictions. The difference between theoretical and practical heat transfer rates can be attributed to several factors. Theoretical calculations assume uniform temperature differences between fluids, which is rarely the case in real-world scenarios due to mixing effects and varying flow dynamics. In contrast, practical calculations factor in the overall heat transfer coefficient U, which includes

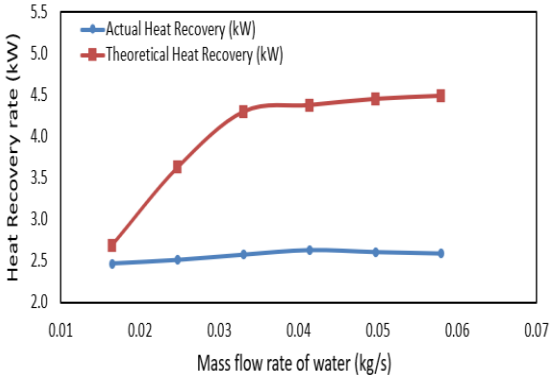

Fig. 9. Actual and predicted heat recovery at different mass flow rates of water

Inefficiencies such as fouling and thermal resistance. These factors are not considered in idealized theoretical models, contributing to the disparities observed in heat transfer rates between theoretical and practical heat recovery rates.

The experimentation results show that the deviation between actual and predicted results is within the range of 15%. Frank Incropera and David Dewitt mentioned in their book Fundamentals of Heat and mass transfer that "Each correlation is reasonable over a certain range of conditions, but for most engineering calculations, one should not expect accuracy to be much better than 20 Percent" [21]. Referring to this statement the deviation in actual and predicted results are within the valid limit.

5. Conclusions

Shell and helical cone coil heat exchangers provide an effective method for harnessing low-grade heat from medium and high-temperature sources, thereby contributing significantly to environmental protection against greenhouse gases and global warming. In experiments, these compact and efficient heat exchangers recovered approximately 45 to 50% of excess heat from exhaust gases, varying with their size. The helical cone coil heat exchanger demonstrated a heat extraction rate of 7.6 kW/m2 and a pressure drop of 4.7 kPa, achieving an effectiveness of 0.58. This highlights its superior performance over traditional tube designs in numerical analyses, making them promising solutions for industrial heat exchange due to enhanced efficiency and practicality.

Experimental results indicated an effectiveness range of 0.45 to 0.6, marking a significant 15 to 20% improvement over conventional shell and tube heat exchangers with similar heat duties. Various cleaning methods can be implemented to mitigate fouling from soot accumulation, with considerations needed for limitations in spiral tube fabrication when modifying designs for diverse industrial requirements. Ultimately, these heat exchangers play a crucial role in conserving energy by capturing otherwise wasted heat. Their innovative design significantly enhances the recovery of low-grade heat, thereby improving process efficiency across sectors such as textiles, food processing, power generation, and HVAC systems. This advanced technology supports green energy initiatives and environmental preservation by efficiently recovering secondary heat from medium to high-temperature sources, underscoring its role as a potent solution for sustainable heat exchange.

Limitation of Study: However, the experimental results presented are based on controlled conditions in a laboratory setting. Implementing these heat exchangers in real-world industrial applications may encounter additional challenges, such as scale-up issues, maintenance requirements, and economic feasibility, which were not fully addressed in this study.

Future Scope: Future research could focus on optimizing these heat exchangers further to enhance performance under varying operational conditions. Advancements in materials and manufacturing techniques hold the potential to overcome current fabrication limitations, thereby expanding the application scope of helical cone coil heat exchangers and enabling more efficient and sustainable energy solutions.

Nomenclature

A	Area for heat transfer, m^2
A_{fl}	Area available for flow, m^2

C_i	Constant in Richard et al. correlation
T	Temperature, ˚C
a	Constant in equation of spiral
Cp	Specific heat, kJ / kg.K
ΔT_{lm}	Log mean temperature difference, ˚C
D	Diameter of shell, m
U_o	Overall Heat Transfer coefficient, W/m^2 K
De	Dean Number
V	Velocity, m/s
v	Volume flow rate m^3/s
d	Diameter of tube, m
f	Friction factor
h	Heat transfer coefficient, W/m^2 K
L	Length of tube for Pancake, m
P	Pressure, bar
p	Pitch
Nu	Nusselt Number
Re	Reynolds Number
q	Total Heat Duty, kW
R	Radius of spiral, m
m	Mass Flow rate, kg/s
Pr	Prandtl number
DH	Mean diameter of cone
DmH	Small diameter of cone
DMH	Big diameter of cone
D1	Big diameter of wooden cone
d1	Small diameter of wooden cone
S_h	Slant height of full cone
s_h	Slant height of wooden mold cone
d_{ho}	Header at outlet
C_c	Heat capacity of cold fluid
C_h	Heat capacity of hot fluid
d	Diameter of the tube used for coil
$\dot{m}$	Mass flow rate (kg/s)
D1	Big diameter of wooden cone
d1	Small diameter of wooden cone

Greek Symbol

K	Thermal conductivity, W/mK
ρ	Density, kg/m^3
μ	Dynamic Viscosity, kg/ms
$\in$	Effectiveness
θ	Angle in radians in case of spiral

Subscript

o	Outlet
w	Water
g	Gas
i	Inlet
c	Cold
cc	Conical coil
e	Exhaust
min	Minimum

Funding Statement

This research did not receive any specific grant from funding agencies in the public, commercial, or not-for-profit sectors.

Conflicts of Interest

The author declares that there is no conflict of interest regarding the publication of this article.

References

[1] LINES, 2012, Helically Coiled Heat Exchangers Offer Advantages.

[2] Acharya, N., Sen, M. and Chang, H.C., 2001. Analysis of heat transfer enhancement in coiled-tube heat exchangers. International

journal of heat and mass transfer, 44(17), pp.3189-3199

[3] Ghorbani, N., Taherian, H., Gorji, M. and Mirgolbabaei, H., 2010. An experimental study of thermal performance of shell-and-coil heat exchangers. International Communications in Heat and Mass Transfer, 37(7), pp.775-781. doi: 10.1016/j.icheatmasstransfer.2010.02.001.

[4] Jouhara, H., Almahmoud, S., Chauhan, A., Delpech, B., Nannou, T., Tassou, S.A., Llera, R., Lago, F. and Arribas, J.J., 2017. Experimental investigation on a flat heat pipe heat exchanger for waste heat recovery in steel industry. Energy Procedia, 123, pp.329-334. doi: 10.1016/j.egypro.2017.07.262.

[5] Tandale, M.S. and Joshi, S.M., 2008, January. Design of heat exchanger for waste heat recovery from producer gas. In Proceedings of the International Conference on Heat and Mass Transfer, pp. 83–88.

[6] Gholamalizadeh, E., Hosseini, E., Jamnani, M.B., Amiri, A. and Alimoradi, A., 2019. Study of intensification of the heat transfer in helically coiled tube heat exchangers via coiled wire inserts. International Journal of Thermal Sciences, 141, pp.72-83. doi: 10.1016/j.ijthermalsci.2019.03.029.

[7] Alimoradi, A. and Veysi, F., 2017. Optimal and critical values of geometrical parameters of shell and helically coiled tube heat exchangers. Case Studies in Thermal Engineering, 10, pp.73-78. doi: 10.1016/j.csite.2017.03.003.

[8] Purandare, P.S., Lele, M.M. and Gupta, R.K., 2015. Investigation on thermal analysis of conical coil heat exchanger. International Journal of Heat and Mass Transfer, 90, pp.1188-1196. doi: 10.1016/j.ijheatmasstransfer.2015.07.044.

[9] Joshi, S.M. and Anand, S.R., 2015, February. Design of conical helical coil heat exchanger for waste heat recovery system. In 2015 International Conference on Technologies for Sustainable Development (ICTSD) (pp. 1-8). IEEE. doi: 10.1109/ICTSD.2015.7095883.

[10] Flórez-Orrego, D., Arias, W., López, D. and Velásquez, H., 2012, June. Experimental and CFD study of a single phase cone-shaped helical coiled heat exchanger: an empirical correlation. In Proceedings of the 25th international conference on efficiency, cost, optimization, simulation and environmental impact of energy systems (ECOS 2012, vol. 1, pp. 375-394)

[11] Zolfagharnasab, M.H., Pedram, M.Z., Hoseinzadeh, S. and Vafai, K., 2022. Application of porous-embedded shell and tube heat exchangers for the waste heat recovery systems. Applied Thermal Engineering, 211, p.118452.

[12] Missaoui, S., Driss, Z., Ben Slama, R. and Chaouachi, B., 2024. Effects of helical condenser coil designs on the heating process of the domestic refrigerator for hot water production: A numerical study. Numerical Heat Transfer, Part A: Applications, 85(3), pp.328-350.

[13] Missaoui, S., Driss, Z., Slama, R.B. and Chaouachi, B., 2022. Effects of pipe turns on vertical helically coiled tube heat exchangers for water heating in a household refrigerator. International Journal of Air-Conditioning and Refrigeration, 30(1), p.6.

[14] Missaoui, S., Driss, Z., Slama, R.B. and Chaouachi, B., 2022. Experimental and numerical analysis of a helical coil heat exchanger for domestic refrigerator and water heating. International Journal of Refrigeration, 133, pp.276-288.

[15] Missaoui, S., Driss, Z., Slama, R.B. and Chaouachi, B., 2021. Experimentally validated model of a domestic refrigerator with an immersed condenser coil for water heating. International Journal of Air-Conditioning and Refrigeration, 29(03), p.2150022.S.

[16] Missaoui, S., Driss, Z., Slama, R.B. and Chaouachi, B., 2021. Numerical analysis of the heat pump water heater with immersed helically coiled tubes. Journal of Energy Storage, 39, p.102547.

[17] Missaoui, S., 2024. Optimized shape design and thermal characteristics investigation of helically coiled tube type heat exchanger. Chemical Engineering Research and Design, 201, pp.96-107.

[18] Coleman, H.W. and Steele, W.G., Experimentation and Uncertainty Analysis for Engineers, Wiley, New York, 1989.

[19] ANSI/ASME, Measurement uncertainty, 1986, Report PTC 19, pp. 1–1985.

[20] Kannadasan, N., Ramanathan, K. and Suresh, S., 2012. Comparison of heat transfer and pressure drop in horizontal and vertical helically coiled heat exchanger with CuO/water based nano fluids. Experimental Thermal and Fluid Science, 42, pp.64-70.

[21] Incropera, F.P., DeWitt, D.P., Bergman, T.L. and Lavine, A.S., 1996. Fundamentals of heat and mass transfer, New York, Wiley. ISBN 10:0471304603 / ISBN 13:9780471304609